School of Natural Sciences and Mathematics
William B. Hanson Center for Space Sciences

Plasma Dynamics Associated with Equatorial Ionospheric Irregularities

UT Dallas Author(s):

Jonathon Matthew Smith
Roderick A. Heelis

Citation:

Smith, J. M., and R. A. Heelis. 2018. "Plasma Dynamics Associated With Equatorial Ionospheric Irregularities." Geophysical Research Letters 45(16): 7927-7932, doi: 10.1029/2018GL078560

AGU100 ADVANCING EARTH AND SPACE SCIENCE

Geophysical Research Letters

RESEARCH LETTER
10.1029/2018GL078560

Key Points:
- Topside depletions seen near and after midnight during solar moderate contain plasma that is drifting strongly downward with the background
- Topside depletions detected near midnight during solar minimum contain plasma that is moving upward within a downward moving background
- Weak vertical drifts that maintain the bottomside altitude while the neutral density decreases aid depletion growth at solar minimum

Correspondence to:
J. M. Smith,
jms074100@utdallas.edu

Citation:
Smith, J. M., & Heelis, R. A. (2018). Plasma dynamics associated with equatorial ionospheric irregularities. *Geophysical Research Letters*, *45*, 7927–7932. https://doi.org/10.1029/2018GL078560

Received 9 MAY 2018
Accepted 16 JUL 2018
Accepted article online 23 JUL 2018
Published online 17 AUG 2018

Plasma Dynamics Associated With Equatorial Ionospheric Irregularities

Jonathon Matthew Smith[1] **and R. A. Heelis**[1]

[1] William B. Hanson Center for Space Sciences, The University of Texas at Dallas, Richardson, TX, USA

Abstract The Communication/Navigation Outage Forecasting System satellite was operational from 2008, a period of deep solar minimum, to 2015, a period of moderate solar conditions. The behavior of the vertical plasma drift and the distribution of plasma depletions during the deep solar minimum of 2009 deviated substantially from the behavior that was observed during the solar moderate conditions encountered by the Communication/Navigation Outage Forecasting System satellite in 2014, which are typical of previous observations. Presented here are observations of the vertical drift of plasma depletions and the background plasma in which they are embedded. We find that depletions detected at local times after 2100 hr during solar minimum are typically found in background drifts that are weakly downward compared to the strongly downward background drifts observed during moderate solar activity levels. Additionally, at solar minimum, the drift within the depletions is upward with respect to the background as compared with observations at the same local times during solar moderate conditions for which the depleted plasma more nearly drifts with the background. We note that weak background plasma drifts observed throughout the night during solar minimum promote the continued growth of depletions that may evolve more slowly or be continuously generated to appear in the topside in the postmidnight hours.

Plain Language Summary The generation of equatorial ionospheric irregularities represents a fundamental plasma process of interest to a broad spectrum of plasma physicists. Interest in the Earth's ionosphere particularly broad and currently active because the evolution of conditions that give rise to the growth of plasma structures is not well understood. In particular many studies of the ionosphere under the recent solar minimum conditions have shown that equatorial plasma structures do not behave in the same way as those seen at more moderate solar activity levels. Various studies have shown that the large-scale dynamics of the ionosphere has a strong influence on the evolution of plasma structures. This work reports on the average properties of the underlying background dynamics of the equatorial ionosphere that exists in the absence and presence of plasma structure. Such information can be broadly utilized to reevaluate instability growth rates as they apply to a variety of different observational conditions. The behavior of ionosphere under very low solar activity levels has been unique and provides opportunities for new insights into the dynamic ionosphere in which irregularities are formed.

1. Introduction

Recent studies of equatorial plasma irregularities have shown that their appearance in the topside ionosphere during the solar minimum period of 2009 is largely confined to postmidnight hours (Heelis et al., 2010; Smith & Heelis, 2017). These studies acknowledged that the absence of topside ionospheric structures in the postsunset period during solar minimum may result from relatively long growth times that prevent their appearance at the earliest local times. However, Smith and Heelis (2017) point out that the increased appearance of postmidnight structures at solar minimum, compared to more moderate levels of solar activity, might indicate that irregularities can also be generated at later local times than would be expected during moderate solar activity. Additionally, these irregularities may continue to drift upward to appear in the topside at even later local times.

The vertical drift of the equatorial plasma has two major influences on the appearance of plasma bubbles in the topside. First, the drift raises and lowers the layer while the layer is being produced during the daytime and while the layer density is decreasing at night. This determines the height of the bottomside and thus the flux tube integrated conductivity and the Pedersen conductivity weighted value of the gravitationally driven

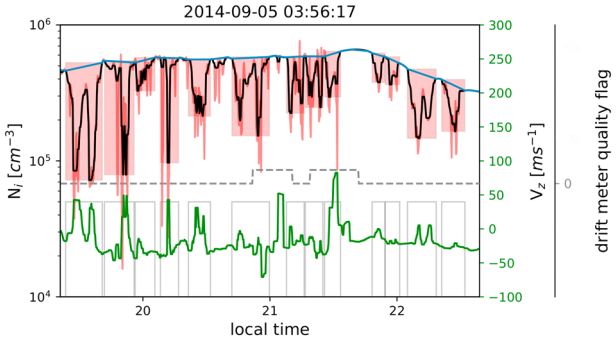

Figure 1. Key parameters used in this work. Top panel shows the raw total ion density profile in red and the filtered density profile in black. Lower panel shows local vertical ion drift in green. The background density identified by the rolling ball is shown in blue. Regions identified as discrete depletions are shown in pink; the same regions in the drift are surrounded by rectangles. The dashed line is the quality flag; here there are some samples with a nonzero quality flag indicating the magnetic torquers on the spacecraft are active.

zonal current. For flux tubes with low apex heights we expect that the meridional wind will have a small influence on the growth of perturbations, since the dip angle remains small at all locations along a flux tube. Thus, we assume that gravity, along with the zonal electric field associated with the vertical drift and the flux tube integrated conductivity, largely determines the growth rate of a perturbation as described in equation (26) of Sultan (1996). For plasma irregularities appearing in the postsunset period near the Jicamarca radar, Fejer et al. (1999) have shown how the vertical plasma drift affects the height of the layer across sunset and have established a threshold condition for which equatorial irregularities are most likely to grow into the topside. Stolle et al. (2008) found that there is a threshold of the vertical plasma drift required for the observation of equatorial spread *F* (ESF) at satellite altitudes. Su et al. (2008) suggested that the seasonal and longitudinal variations in the magnitude of the vertical plasma drift at sunset is sufficient to explain the global distribution of ESF occurrence due to the strong correlation between vertical drift at sunset and ESF occurrence. Huang and Hairston (2015) examined the relationship between the vertical plasma drift near sunset and the subsequent appearance of plasma depletions observed by the Communication/Navigation Outage Forecasting System satellite. They found that a larger magnitude for the prereversal enhancement (PRE) was associated with the more frequent occurrence of deep plasma depletions in the topside equatorial ionosphere in the postsunset sector. Huang (2018) further suggests that the occurrence probability for spread *F* detected by satellites in the topside increases linearly with the strength of the PRE. Here we investigate the relationship between the vertical ion drift and the appearance of plasma bubbles in the topside equatorial ionosphere in the postmidnight sector. This is particularly relevant at solar minimum, where we have established that deep bubbles are more prominent in the postmidnight sector than at moderate levels of solar activity and are perhaps actively produced in this period in addition to their drifting from earlier local times.

2. Observations

This work utilizes the same database of ionospheric depletions that is described by Smith and Heelis (2018). Measurements of ionospheric density are made at a 1-Hz rate by instruments as a part of the Coupled Ion Neutral Dynamics Investigation aboard the Communication/Navigation Outage Forecasting System satellite. The data span the years from 2008 to 2015 and include a deep solar minimum in 2009 when the average solar radio flux is 72.1 $\times 10^{-22}$ W·m^{-2}·Hz^{-1} as well as a moderate solar activity period in 2014 when the average solar radio flux is 143.8 $\times 10^{-22}$ W·m^{-2}·Hz^{-1}. Each of these years provides an opportunity to examine the nature of the plasma depletions observed in the topside during a solar minimum and a solar moderate period. Throughout this discussion the observations during 2009 and 2014 are used to represent conditions at solar minimum and solar moderate respectively.

Figure 1 shows an example of the measured total plasma density and vertical ion drift during a nighttime pass across the equatorial topside. In order to focus solely on large-scale plasma structures, the original samples, shown in red, of plasma density are filtered to remove small-scale fluctuations with scale sizes less than 50 km as indicated by the black curve in the top panel of Figure 1. A rolling ball with a characteristic scale size of $\approx$ 550 km is then applied to this time series to identify the background density profile shown in blue (Smith & Heelis, 2018). The rolling ball approach used here is performed by obtaining the convex hull of the set of time series points. The top half of this convex hull identifies the upper envelope of the time series, which defines the background density profile. The depletions, simply identified by deviations from the background, are highlighted in pink and span a range of widths from approximately 200–500 km. This procedure permits variations in the density and drift to be examined simultaneously within and outside depleted plasma regions. In the bottom panel the vertical drift is shown in green and rectangles are drawn to show the vertical ion drift within the identified depletions. A data quality flag, with values ranging from 0 to 9, shown by the dashed line through Figure 1, indicates regions where very low O^+ density, active magnetic torquers on the spacecraft, sunlight shining into the instrument aperture, and/or the satellite telemetry may compromise the measurements. Data quality flag values of 0 indicate the very best quality data and after depletions have been

identified only those depletions with all zero quality flag values are considered. The depletions lost due to this selection still allow a robust data set with a statistically significant sample size of 7302 in 2009 and 20430 in 2014. For each discrete depletion we record the background density N_b and the background vertical drift V_{bdep}, as the average of the background quantities at each edge of the depletion, the minimum depletion density N_{min}, the depletion depth $(N_b - N_{min})/N_b$, and the maximum value of the drift inside the depletion, V_d. After imposing the restrictions to ensure that the drift data are not adversely affected by large variations associated with plasma densities less than 10^3 cm^{-3}, we investigated the behavior of the vertical ion drift and the associated appearance of plasma depletions.

To examine the dynamic state of the topside ionosphere associated with plasma depletions, we produce hourly median values of the background vertical drift (V_b), where the data quality allows and note the presence of depletions with depths greater than 50% occurring within the three hours beginning with the hour of drift observation. We distinguish between hours when no depletions are detected and when at least one depletion is detected in the designated local time span as *calm* and *depleted*, respectively.

The data for all seasons are considered for the years 2009 and 2014. However, since the local time pattern of the vertical drift and occurrence of ionospheric structures are seasonally dependent the descriptions for calm and depleted periods also reflect differences between the seasons when calm and depleted conditions are dominant. Calm and depleted seasons are different at different longitudes primarily due to the magnetic declination (Tsunoda, 1985). Thus, the data for each year are divided broadly into longitude regions with different magnetic declinations. We refer to them as the African sector from −15° to 60°, where the magnetic declination is weakly positive; the Indian sector from 60° to 130°, where the declination is weakly negative; the Pacific sector from 130° to −75°, where the declination is positive; and the South American sector from −75° to −15°, where the declination is negative.

We investigate the difference in the observed plasma dynamics in the topside equatorial region during moderate solar activity, when plasma depletions are predominantly seen in the postsunset period and during low solar activity, when plasma depletions are predominantly seen in the postmidnight period. Thus, from each orbit we focus on local times from 1800 to 0600 hr. Over this local time range the magnetic latitude of the observations here may change significantly between about −20° and 20° due to the satellite's orbit. While the presence of bubbles may be detected over this entire latitude range, in determining the vertical ion drift we restrict our attention to data taken within 10° of the magnetic equator, where the inclination is small and the local vertical drift measured by the Coupled Ion Neutral Dynamics Investigation Drift Meter can be used to confidently specify the E×B drift of the plasma.

3. Results

Figure 2 shows median values of the background vertical plasma drift as a function of local time in each longitude sector and solar activity level. The behavior observed in 2014 and 2009 is shown in the top and bottom panels, respectively. Each panel depicts the designated longitude region with calm hours shown in blue and depleted hours shown in red. The bars represent the 75th percentile for each median and the sample size for each median is shown in the corresponding color above and below the curve. Local times are omitted when fewer than 10 samples are available. For each longitude sector the seasonal dependence of depletion occurrence largely separates the calm and depleted profiles by season. This seasonal-longitude dependence is not our focus here as we are simply investigating the difference between drifts occurring in the presence and absence of depletions, regardless of season.

During solar moderate conditions in 2014 the drift behavior of both calm and depleted hours is generally consistent with the drift patterns observed and modeled by Fejer et al. (2008). The presence of depletions during postsunset hours is associated with a PRE in the ion drift in all longitude sectors, while the reversal to a downward drift at earlier local times than those seen for depleted hours is characteristic of all occasions where depletions are not seen. Between 2100 and 2400 hr the background drifts for calm and depleted hours are identical, indicating that the downward drift is effective in suppressing the further evolution of depletions from the bottomside. The equality of the drift profiles for calm and depleted conditions continues to predawn in the Pacific and Indian sectors even while the downward drift weakens, suggesting that no further growth of depletions occurs after the postsunset hours. In the African and South American sectors, however, the

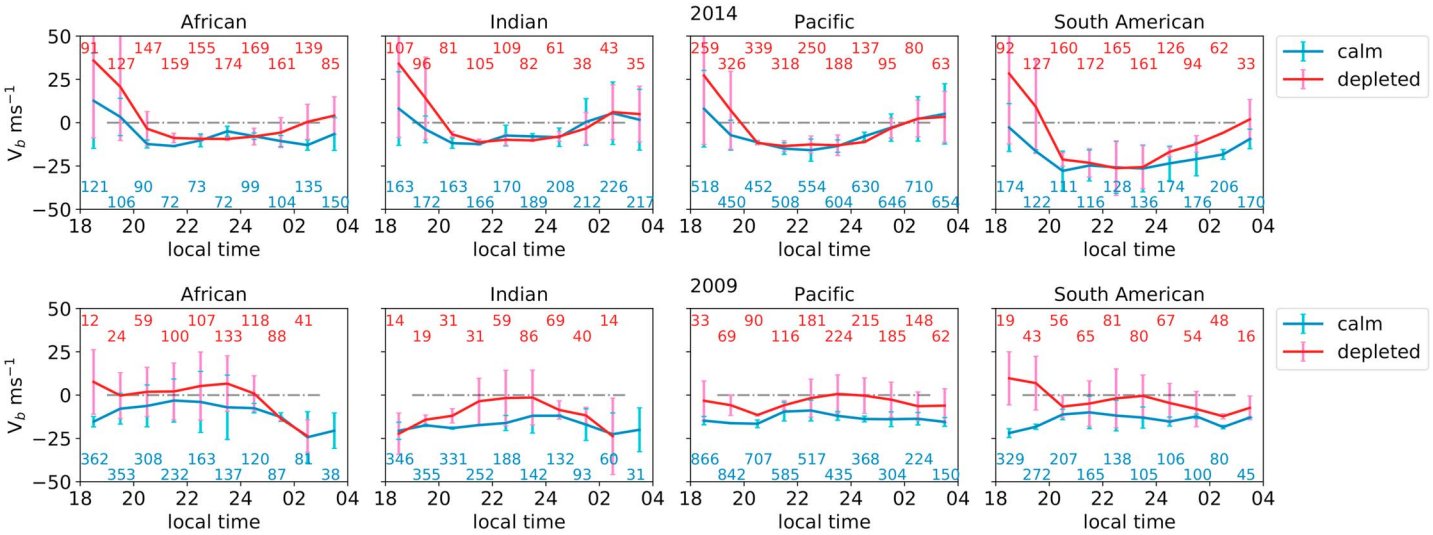

Figure 2. Median background vertical drifts as a function of local time for each longitude region. Depleted hours are shown in red, while calm hours are shown in blue. The bars show the 75th percentile for each median value. The numbers in red and blue at the top and bottom of each panel are the number of points over which a median was taken for each hour.

maintenance of larger downward drifts suppresses the appearance of postmidnight depletions, suggesting that the appearance of postmidnight depletions in these sectors during moderate solar conditions is related to additional growth processes during this period.

For solar minimum conditions in 2009, in the absence of depletions the vertical drift is almost constant throughout the period from 1800 to 0400 hr and is downward with speeds near 20 m/s, presumably sufficient to suppress positive growth produced by the gravitationally driven current. The background density in which depletions are embedded can be low in the postmidnight hours, leading to increased uncertainty in the determination of the vertical drift. Therefore, the behavior of the background drift in this period should be viewed with caution. Nevertheless, in the presence of depletions the downward drift is reduced to values less than 10 m/s in all longitude regions except at postsunset and presunset local times in the Indian sector. In the postmidnight sector, the vertical drift in the presence of plasma depletions remains weakly downward, less than 5 m/s, in the Pacific and South American sectors. However, in the African and Indian sectors the postmidnight drift becomes more negative and approaches the conditions seen in the absence of depletions. In the presence of depletions, we note that the vertical drift in most longitude sectors is weak and relatively constant from 2200 to 0200 hr. Thus, the gravitationally driven current could provide a growth rate large enough to overcome a weak downward drift suggesting these depletions could be actively moving into the topside.

To present further evidence for the active evolution of plasma depletions into postmidnight hours during solar minimum, we examine the plasma velocity within depleted regions. As the depletion develops, the plasma flow within the depletion evolves nonlinearly (Ossakow & Chaturvedi, 1978), but Hanson and Bamgboye (1984) have provided a simple analysis that relates the plasma drift inside the depletion to the background drift based on the ratio of the flux tube integrated Pedersen conductivity inside and outside of the depletion. Thus, plasma moving upward indicates the active evolution of the depletion, while so-called fossil depletions will drift with the background plasma. Figure 3 shows the vertical plasma drift internal to depletions in each longitude sector for 2014 and 2009. These drifts are organized into one hour bins and the median and 75th percentiles of the internal drift (V_d) for depletions occurring in that hour are plotted as in figure 2. During 2009 when depletions are embedded in background densities that can be less than 10^4 cm^{-3}, it is often not possible to measure the vertical drift near the depletion minimum. In this case the vertical drift for a depletion is specified as the maximum drift value of all points within a depletion where the density exceeds 10^4 cm^{-3}. During 2014, this limitation is minimal since most depletions are embedded in background densities that are larger than 10^4 cm^{-3}.

We find that during 2014 (red curve), the plasma in most depletions moves rapidly upward in the postsunset hours until 2100 hr and subsequently moves downward or very weakly upward thereafter. This behavior is

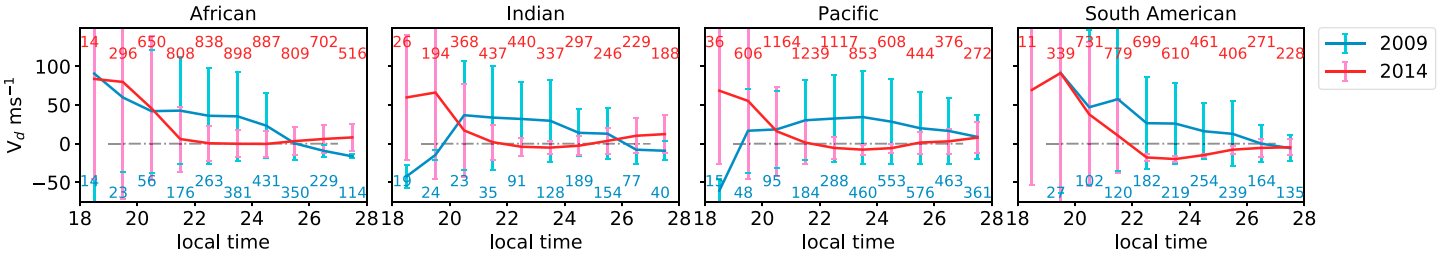

Figure 3. Median of the maximum internal vertical drift of depletions as a function of local time for each longitude region in 2009 and 2014. Depletions considered here are confined within 10° of the magnetic equator. The bars show the 75th percentile for each median value. The numbers in red and blue at the top and bottom of each panel are the number of points over which a median was taken for each hour.

largely independent of longitude and is consistent with the rapid postsunset evolution of depeletions into the topside and subsequent motion with the background plasma as a so-called fossil depletion. During 2009 (blue curve), depleted plasma motion in the postsunset period in the African and South American sectors is almost the same as that seen during 2014. The point of emphasis here is that it does not occur frequently. In the hours following 2100 hr, however, the depleted plasma drift in 2009 remains substantially upward throughout the period beyond local midnight, suggesting that the depletions are actively evolving, while the median background drift accompanying the depletions and shown in Figure 2, is weakly downward.

4. Discussion

Depletions observed above the *F* peak evolve from perturbations in the bottomside that rise into the topside over time scales from minutes to hours. Thus, the local time at which ionospheric irregularities appear at different altitude regions can be quite different and is dependent on when the depletions are seeded and the time evolution of the vertical and zonal ion drifts.

At later local times during solar moderate conditions, the bottomside density gradient with altitude steepens as recombination removes ions. However, depletions originating in the bottomside are unlikely to grow into the topside because the vertical drift is strongly downward and the associated zonal current opposes the current associated with the gravitational force, thereby suppressing the growth of new depletions. This is illustrated here by noting that depletions observed in the topside at and after local midnight contain plasma that is drifting with the background. Therefore, the plasma is not actively convecting upward, as would be the case for an evolving depletion in which the Pedersen conductivity is lower than the background.

During the solar minimum period of 2009, plasma depletions appear in the topside despite the absence of strong vertical drifts like those seen during moderate solar activity following a PRE. In 2009 we also find evidence that the plasma within depletions is moving upward with respect to the background plasma during postmidnight hours, indicating that the depletions are continuing to evolve from the bottomside. Thus, in the presence of near-zero drifts throughout a significant period of the night, there are processes that maintain reasonable growth rates. While there is no significant PRE signature in the vertical plasma drift, there is also no large reversal from an upward to a downward drift. Thus, a more uniform, however, weak drift, which does not entirely suppress the contribution to the *R-T* linear growth rate from the gravitational current, permits a longer evolution time for depletions. During 2009, depletions are generally observed in the topside at later local times than those depletions seen during moderate and high solar activity (Smith & Heelis, 2017).

Small vertical drifts, like those seen in 2009, maintain the *F* layer peak height during the night when the vertical plasma drift strongly controls the height of the *F* peak. Thus, during solar minimum vertical drifts with low magnitudes are associated with a relatively stationary *F* peak height. In this case the decay of the bottomisde by recombination tends to raise the altitude at which the bottomside altitude gradient in density is a maximum. The resulting increase in the gravitational current increases the growth rate from that expected at moderate solar activity for later local times during which a downward drift would lower the altitude of the bottomside density gradient. Finally, the sustained small vertical drifts through midnight allow a positive growth rate to be maintained while the neutral atmosphere cools. This reduces the neutral scale height, thereby reducing the neutral density at the bottomside plasma density gradient and further increases the depletion growth rate.

A detailed computation of the flux tube integrated linear growth rate is described by Ajith et al. (2016) for June solstice conditions in the longitude region between 60° and 120° during moderate solar activity. Under these conditions the normally downward drift throughout the night becomes only weakly downward around midnight and a local enhancement in the growth rate for plasma irregularities in the bottomside is derived. A computation of the flux tube integrated linear growth rate under solar minimum conditions near 75° is described by Zhan and Rodrigues (2017). Under the weak downward drifts observed concurrently with fully developed ESF the modeled growth rates were positive. This growth rate can be enhanced by the action of equatorial meridional neutral winds.

We have little insight into any systematic changes in the *F* region neutral winds from solar maximum to solar minimum, but our observations show that weak or even upward drifts exist over substantially extended local time periods through the night at solar minimum. Thus, at solar minimum it is possible that plasma irregularities can grow continuously after sunset and be observed continuously at later local times through the night.

5. Conclusions

Examination of the vertical ion drift accompanying the appearance of plasma depletions shows a distinct difference in behavior that is dependent on solar activity. During moderate solar activity the PRE enhancement of upward plasma drift is associated with depletions that appear in the postsunset local time sector and subsequently drift downward with the background in the postmidnight sector. However, depletions may continue to evolve in the postmidnight sector if vertical drifts remain low in magnitude, as is the case during solar minimum. The maintenance of weak vertical plasma drifts during the night at solar minimum also aids the maintenance of the *F* peak, while the bottomside plasma density gradient steepens and the neutral density at the bottomside decreases as the atmosphere cools. All these factors combine to produce a modest growth rate such that plasma structures may be continuously generated and move upward to be continuously observed in the topside throughout the night.

Acknowledgments
The C/NOFS mission is supported by the Air Force Research Laboratory, the SMC Defense Weather Systems Directorate, the Department of Defense Space Test Program, the National Aeronautics and Space Administration, the Naval Research Laboratory, and The Aerospace Corporation. Work at the University of Texas at Dallas was supported by NASA grant NNX15AT31G. The solar ionizing flux ($F_{10.7}$) data are available via the Space Physics Data Facility OMNIWeb interface. The link to this database from OMNI2 is from https://omniweb.gsfc.nasa.gov/form/dx1.html. The C/NOFS CINDI data are available from https://cdaweb.sci.gsfc.nasa.gov/cdaweb/sp_phys/.

References

Ajith, K. K., Ram, S. T., Yamamoto, M., Otsuka, Y., & Niranjan, K. (2016). On the fresh development of equatorial plasma bubbles around the midnight hours of June solstice. *Journal of Geophysical Research: Space Physics*, *121*, 9051–9062. https://doi.org/10.1002/2016JA023024

Fejer, B. G., Jensen, J. W., & Su, S.-Y. (2008). Quiet time equatorial *F* region vertical plasma drift model derived from ROCSAT-1 observations. *Journal of Geophysical Research*, *113*, A05304. https://doi.org/10.1029/2007JA012801

Fejer, B. G., Scherliess, L., & de Paula, E. R. (1999). Effects of the vertical plasma drift velocity on the generation and evolution of equatorial spread *F*. *Journal of Geophysical Research*, *104*(A9), 19,859–19,869. https://doi.org/10.1029/1999JA900271

Hanson, W. B., & Bamgboye, D. K. (1984). The measured motions inside equatorial plasma bubbles. *Journal of Geophysical Research: Space Physics*, *89*(A10), 8997–9008. https://doi.org/10.1029/JA089iA10p08997

Heelis, R. A., Stoneback, R., Earle, G. D., Haaser, R. A., & Abdu, M. A. (2010). Medium-scale equatorial plasma irregularities observed by Coupled Ion-Neutral Dynamics Investigation sensors aboard the Communication Navigation Outage Forecast System in a prolonged solar minimum. *Journal of Geophysical Research*, *115*, A10321. https://doi.org/10.1029/2010JA015596

Huang, C.-S. (2018). Effects of the postsunset vertical plasma drift on the generation of equatorial spread *F*. *Progress in Earth and Planetary Science*, *5*, 3. https://doi.org/10.1186/s40645-017-0155-4

Huang, C.-S., & Hairston, M. R. (2015). The postsunset vertical plasma drift and its effects on the generation of equatorial plasma bubbles observed by the C/NOFS satellite. *Journal of Geophysical Research: Space Physics*, *120*, 2263–2275. https://doi.org/10.1002/2014JA020735

Ossakow, S. L., & Chaturvedi, P. K. (1978). Morphological studies of rising equatorial spread *F* bubbles. *Journal of Geophysical Research: Space Physics*, *83*(A5), 2085–2090. https://doi.org/10.1029/JA083iA05p02085

Smith, J., & Heelis, R. A. (2017). Equatorial plasma bubbles: Variations of occurrence and spatial scale in local time, longitude, season, and solar activity. *Journal of Geophysical Research: Space Physics*, *122*, 5743–5755. https://doi.org/10.1002/2017JA024128

Smith, J. M., & Heelis, R. A. (2018). The plasma environment associated with equatorial ionospheric irregularities. *Journal of Geophysical Research: Space Physics*, *123*, 1583–1592. https://doi.org/10.1002/2017JA024933

Stolle, C., Lühr, H., & Fejer, B. G. (2008). Relation between the occurrence rate of ESF and the equatorial vertical plasma drift velocity at sunset derived from global observations. *Annales Geophysicae*, *26*, 3979–3988. https://doi.org/10.5194/angeo-26-3979-2008

Su, S.-Y., Chao, C. K., & Liu, C. H. (2008). On monthly/seasonal/longitudinal variations of equatorial irregularity occurrences and their relationship with the postsunset vertical drift velocities. *Journal of Geophysical Research: Space Physics*, *113*, A05307. https://doi.org/10.1029/2007JA012809

Sultan, P. J. (1996). Linear theory and modeling of the Rayleigh-Taylor instability leading to the occurrence of equatorial spread *F*. *Journal of Geophysical Research*, *101*(A12), 26,875–26,891. https://doi.org/10.1029/96JA00682

Tsunoda, R. T. (1985). Control of the seasonal and longitudinal occurrence of equatorial scintillations by the longitudinal gradient in integrated *E* region Pedersen conductivity. *Journal of Geophysical Research*, *90*(A1), 447–456. https://doi.org/10.1029/JA090iA01p00447

Zhan, W., & Rodrigues, F. S. (2017). June solstice equatorial spread *F* in the american sector: A numerical assessment of linear stability aided by incoherent scatter radar measurements. *Journal of Geophysical Research: Space Physics*, *123*, 755–767. https://doi.org/10.1002/2017JA024969